NASA TECHNICAL NOTE

MEASUREMENT OF ION AND ELECTRON DENSITIES OF ELECTRON-BOMBARDMENT ION-THRUSTOR BEAM

by Dale W. Cooper and Perry W. Kuhns

Lewis Research Center
Cleveland, Ohio

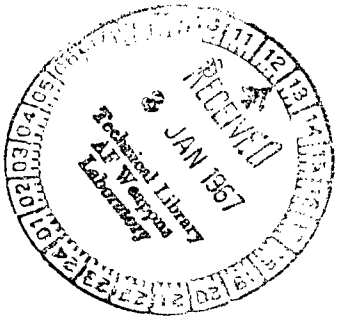

NATIONAL AERONAUTICS AND SPACE ADMINISTRATION • WASHINGTON, D. C. • DECEMBER 1966

NASA TN D-3761

MEASUREMENT OF ION AND ELECTRON DENSITIES OF ELECTRON-BOMBARDMENT ION-THRUSTOR BEAM

By Dale W. Cooper and Perry W. Kuhns

Lewis Research Center
Cleveland, Ohio

NATIONAL AERONAUTICS AND SPACE ADMINISTRATION

For sale by the Clearinghouse for Federal Scientific and Technical Information
Springfield, Virginia 22151 – Price $1.00

MEASUREMENT OF ION AND ELECTRON DENSITIES OF ELECTRON-BOMBARDMENT ION-THRUSTOR BEAM

by Dale W. Cooper and Perry W. Kuhns

Lewis Research Center

SUMMARY

Measurements in both the transverse and the longitudinal directions were taken of an ion-thrustor beam with Langmuir and current probes. These measurements resulted in transverse and longitudinal profiles of electron and ion densities. A comparison was made at the beam centerline between Langmuir probe, current-probe, and microwave-interferometer measurements. The measurements agreed to within ±10 percent.

INTRODUCTION

When ion thrustor configurations are being tested, it is of value to have as complete a knowledge as possible of the characteristics of the ion-thrustor beam. In future applications, when a number of these thrustors are mounted together, such knowledge will aid in the determination of not only the amount and effect of coupling between the thrustor beams but also the completeness of neutralization.

Two types of instruments are of value for measuring the characteristics of ion beams: instruments outside the beam, which integrate over a path through the thrustor beam, and probes for point measurements. The microwave interferometer, which is an integrating instrument, has not been successfully employed previously on ion-thrustor beams because of the low number density and the correspondingly small phase shift. Langmuir probes are difficult to use on ion thrustors because their small diameters result in probe melting and because of the deposition of mercury or cesium on the probe insulator. Current or "button" probes are commonly used in thrustor diagnostics.

In the work reported herein, the microwave interferometer and the Langmuir and current probes were all used. The results are compared, and the sources of error are considered. Measurements were made at one area downstream from the thrustor for comparison of the three techniques, and profile measurements normal to the beam

centerline were made for comparison of the two types of probes.

SYMBOLS

A_c	current probe area, cm
A_L	Langmuir probe area, cm^2
e	particle charge, C
f	frequency, Hz
I_c	current probe current, A
I_e	electron current, A
I_i	ion current, A
I_L	Langmuir probe current, A
J	current density, A/cm^2
k	Boltzmann constant, 1.38×10^{-23} joule per ^oK
m	particle mass, kg
n	particle number density per cubic centimeter
n_{cl}	particle number density per cubic centimeter at centerline
P	total microwave power, mW
P_1	microwave power in reference arm, mW
P_2	microwave power in plasma arm, mW
r	radial distance, cm
T	temperature, V
VSWR	voltage standing wave ratio
V_c	current probe voltage, V
V_L	Langmuir probe voltage, V
V_{net}	net acceleration voltage, V
V_s	space potential, that is, knee in Langmuir probe characteristic curve
x	distance along microwave path, cm
$\Delta\theta$	phase change due to free electrons, rad
$\Delta\theta'$	phase change measured experimentally, rad

ν velocity, cm/sec

Superscripts:

$+$ ion

$-$ electron

THRUSTOR

The thrustor used was a modified electron-bombardment ion thrustor (fig. 1, refs. 1 and 2) that used argon gas as a propellant, thus eliminating the need for a boiler and periodic cleaning of the vacuum system. The filament structure was also modified for simultaneous use of four filaments, thus prolonging filament life (fig. 2).

In the modified electron-bombardment ion thrustor, the propellant is diffused through the distributor into the ionization chamber, where it is bombarded by electrons and ionized. The ionization chamber consists of the filament section and a cylindrical anode with a perforated metal plate, called the screen, at one end. An electromagnet provides an axial magnetic field that confines the electrons emitted by the filament and increases the ionization of the argon gas. A plasma is formed by this ionization process, and the ions are then diffused to the screen where they are extracted by an electric field established between the screen and accelerator plates. The accelerator is a second

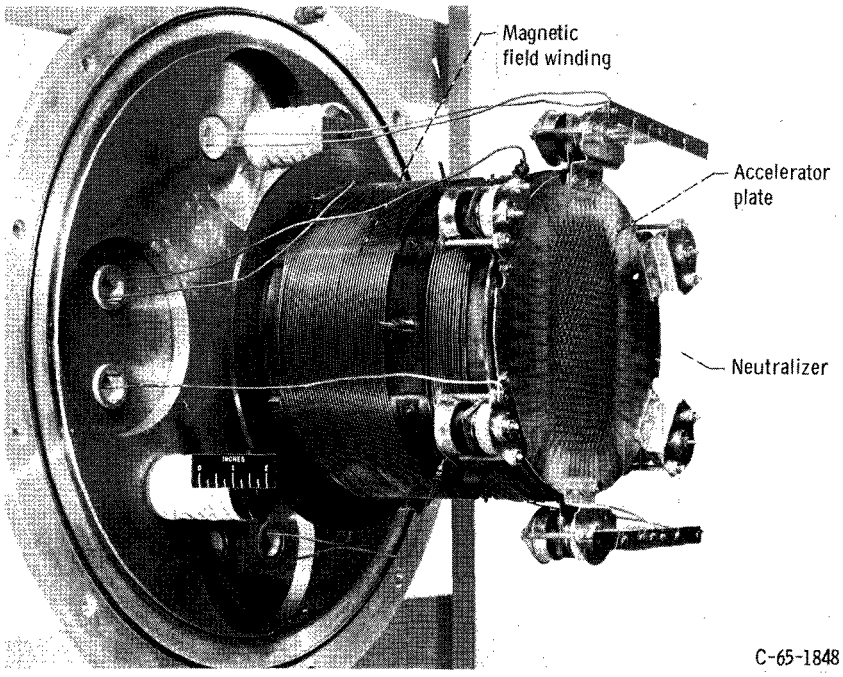

Figure 1. - Ion thrustor.

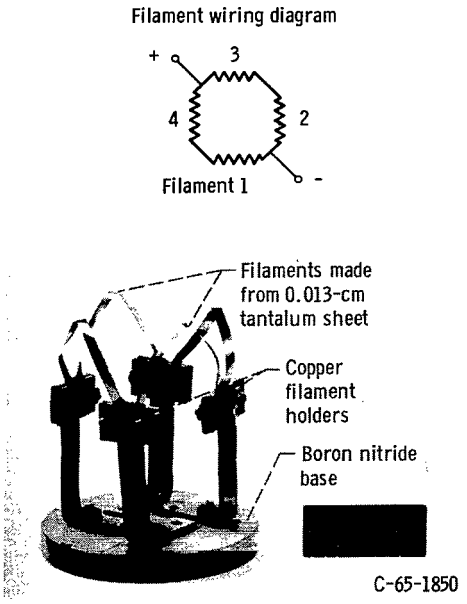

Figure 2. - Thrustor ionizing filament.

perforated plate, separated from the perforated screen by ceramic insulating balls.

In this experiment, the anode was 20.3 centimeters in diameter and 14.0 centimeters in length, and the axial magnetic field was 25 gauss (fig. 1). The screen and accelerator plates were made of 0.130-centimeter-thick molybdenum, match-drilled with 0.476-centimeter-diameter holes arranged in 0.635-centimeter equilateral triangles separated by 0.318 centimeter. The ion-beam exit holes were arranged in a rectangular pattern 10.2 centimeters wide and 17.8 centimeters long.

The thrustor was operated on an accel-decel mode with a total acceleration of 4000 volts and a net acceleration of 2000 volts. When the thrustor is operating, the neutralizer electron current I_e is made equal to the thrustor ion current I_i, thereby ensuring that the neutralization is provided by the neutralizer electrons. The thrustor was operated from five power supplies shown schematically in figure 3; typical operating characteristics are shown in the same figure.

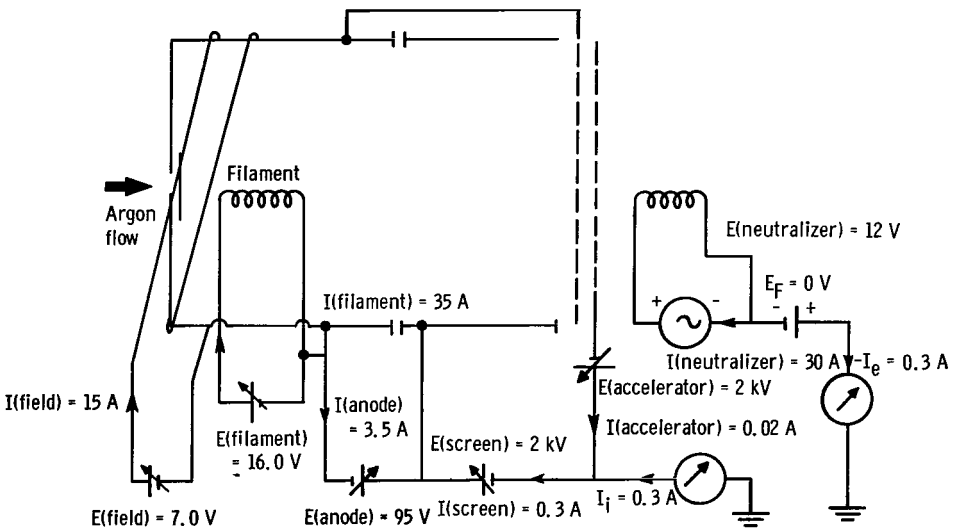

Figure 3. - Ion thrustor wiring diagram. Tank pressure; 4×10^{-5} torr; argon flow rate, 3.0×10^{-4} gram per second; magnetic field, 25 gauss. Values of voltage and current are those incurred during typical engine performance.

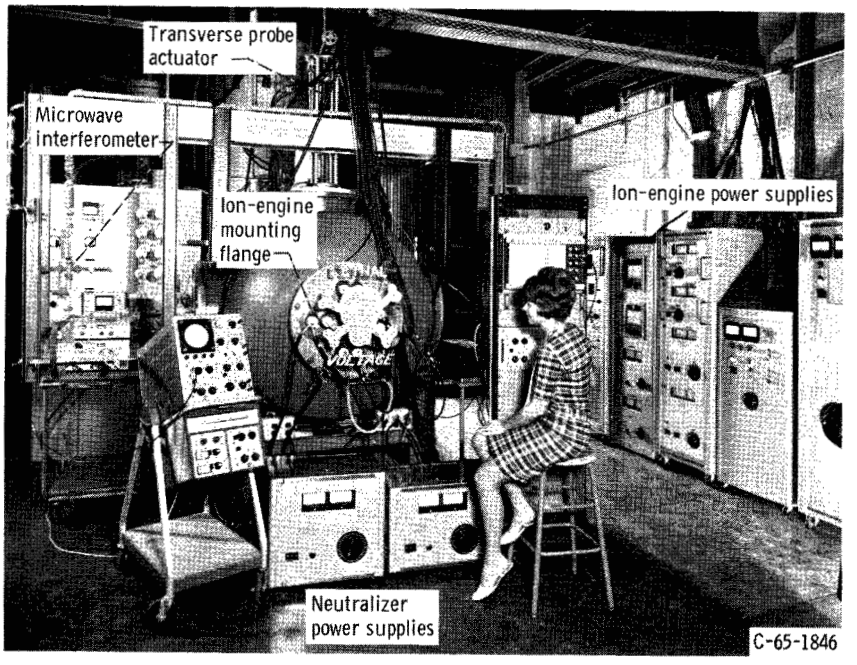

Figure 4. - Test facility at Lewis.

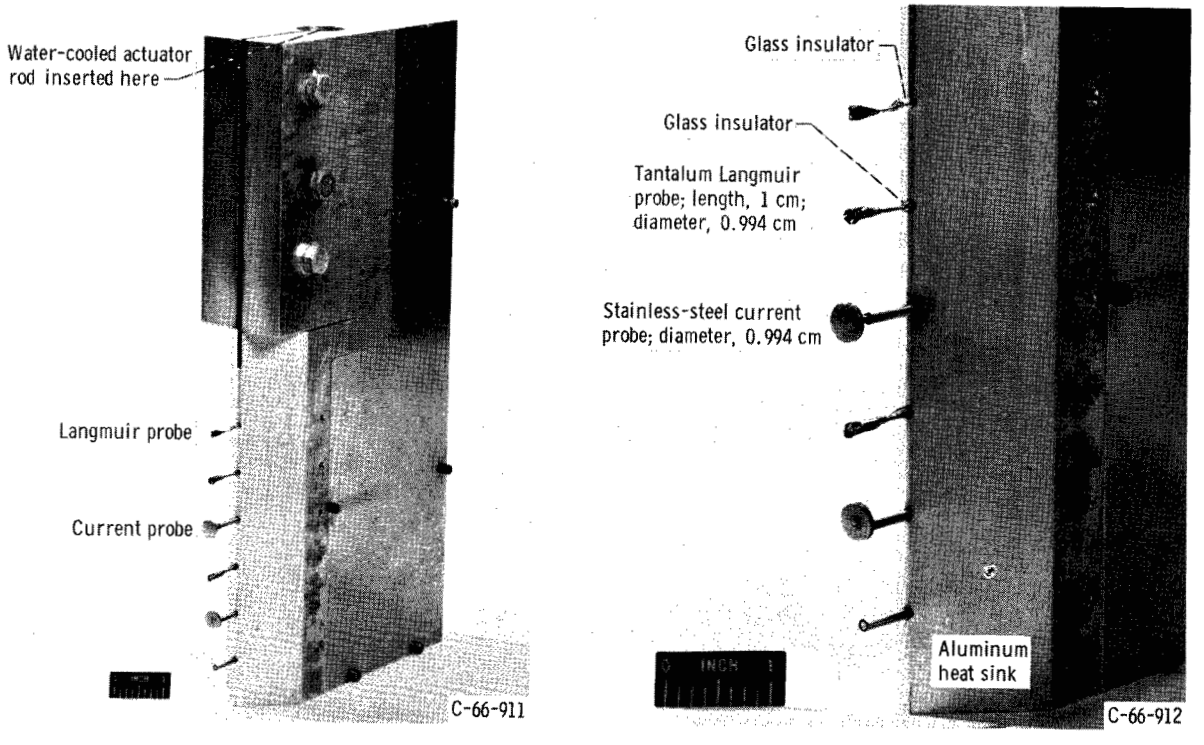

Figure 5. - Current and Langmuir probes used on transverse actuator.

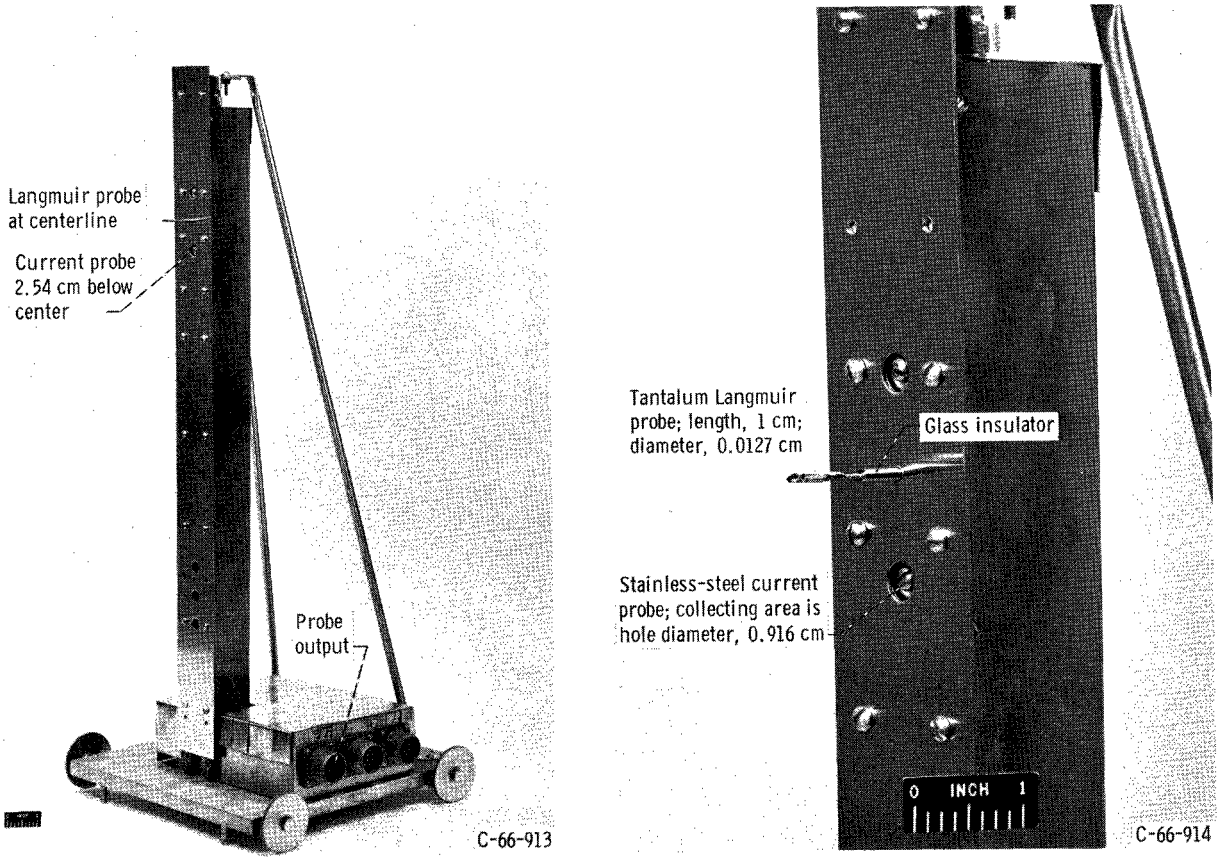

Figure 6. - Current and Langmuir probe cart for downstream measurements.

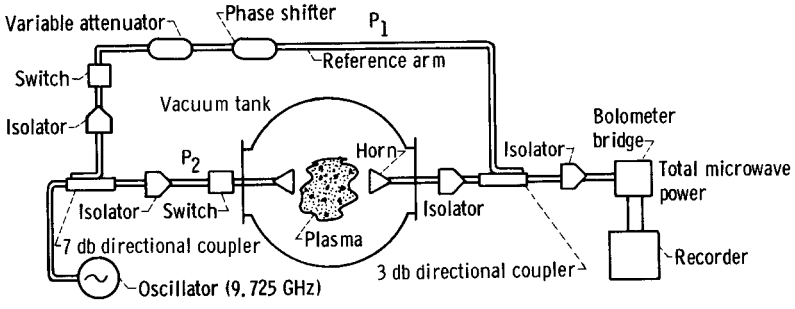

Figure 7. - Schematic diagram of microwave interferometer.

TEST FACILITY

A photograph of the test facility is shown in figure 4. The thrustor was exhausted into a test tank 1.3 meters in diameter and 2 meters in length. This tank was continuously pumped through a 60-centimeter port opposite the ion engine by five diffusion pumps. The pumps used silicon oil and had water-cooled baffles. In addition, the ion-engine beam impinged on a water-cooled plate and there was a liquid-nitrogen-cooled finger in the test tank. The diffusion pumps maintained a pressure of 3×10^{-5} to 6×10^{-5} torr at mass flow rates of 2.5×10^{-4} to 4×10^{-4} gram per second. The blank-off pressure of the system was 3×10^{-6} torr.

Measurement probes were mounted in two ways. Langmuir and current probes were mounted on a vertically moving probe actuator (figs. 4 and 5) that gave continuous readings from 35 centimeters above to 20 centimeters below the centerline. This probe station was 26.7 centimeters downstream from the ion-thrustor exit. The engine and mount could be rotated 90° so that two sets of readings could be made at right angles to each other, yielding height and width profiles.

The second method of mounting had the Langmuir and current probes on a movable rake (fig. 6) so that measurements could be taken transversely to the beam, in a vertical direction, giving readings up to 76 centimeters downstream from the engine exit.

Microwave interferometer (fig. 7) measurements were taken in a horizontal direction, transversely to the beam, and 26.7 centimeters downstream from the ion-engine exit.

INSTRUMENTATION AND MEASUREMENT RELATIONS

Current Probes

The current or button probe is a planar probe that measures direct ion impingement. The bias for this probe was set at -135 volts to repel electrons. The ions were collected to give a thrustor-beam current density from which an ion number-density profile was calculated. The electron saturation region or positive bias is not attractive for this measurement because of the high electron mobility.

The ion current density is given by

$$J^{+} = \frac{I_c}{A_c} \tag{1}$$

from which the ion number density n^+ may be obtained by

$$n^+ = \frac{I_c}{\nu^+ e^+ A_c}$$

The ions in the beam were accelerated through a net potential of 2000 volts so that any ion should have had the theoretical ion velocity given by

$$\nu^+ = 2.2\times10^5 \sqrt{V_{net}} \text{ cm/sec}$$

for argon and

$$\nu^+ = 9.85\times10^6 \text{ cm/sec}$$

for V_{net} = 2000 volts.

In the present study, for purposes of comparison of measurement methods, the beam axial velocity was assumed constant (refs. 3 and 4) making the particle number density proportional to the measured ion current density.

The transverse current probes, shown in figure 5, were stainless steel and were 0.994 centimeter in diameter. The cart current probes, shown in figure 6, were stainless-steel collectors whose collecting area of 0.916 centimeter in diameter was the shadow from the hole in the grounded shield on the cart frame.

Langmuir Probes

The electron density was calculated by using the equations of Langmuir (ref. 5) for probes in the electron saturation region. Since a low-density plasma was measured (approximately 10^8 electrons/cm^3), a thick sheath probe model was assumed, collisions in the plasma were neglected, and electron orbital motion was taken into account. A necessary physical constraint was that the probe radius must be smaller than the Debye length for the theory to remain valid (ref. 5).

From Langmuir (ref. 5), the solution for the probe current in a Maxwellian gas in the electron saturation region yields, for a cylindrical probe,

$$I_L^2 = \frac{(2\times10^{-4})A_L^2 e^2 (n^-)^2}{\pi^2 m^-} \left(-eV_L + kT\right) \qquad (2)$$

The equation for electron number density is obtained by differentiating equation (2) with respect to V_L as follows:

$$n = \frac{3.33\times10^{11}}{A_L}\sqrt{\frac{dI_L^2}{dV_L}} \simeq \frac{3.33\times10^{11}}{A_L}\sqrt{\frac{\Delta I_L^2}{\Delta V_L}} \tag{3}$$

If I_L^2 is plotted as a function of V_L, the intercept of this line at $I = 0$ gives the value of e/kT if V_S, the space potential, is known (ref. 6). Therefore, the electron temperature may also be obtained from the data in the electron saturation region.

The transverse Langmuir probes (fig. 5) were made of molybdenum wire with a diameter of 0.013 centimeter, a length of 1 centimeter, and a radius to Debye length ratio of 0.28 for an electron temperature of 0.5 electron volt. The Langmuir probe in the movable cart (fig. 6) had the same geometry as the transverse Langmuir probes. The electron density was measured at a probe bias of from 22.5 to 45 volts above ground, which was in the electron saturation region that began at about 7 volts, as determined from continuous plots of the Langmuir probe current as a function of voltage.

Microwave Interferometers

The measured phase change is dependent on the electron density and the density profile. The microwave interferometer (fig. 7) measured the phase change between paths 1 and 2. If electron collisions can be neglected, the relation between the phase change in the beam path and the electron density along the microwave path is given by (refs. 7 and 8)

$$\int \bar{n}\, dx \simeq 7.45\times10^2\, f\left|\frac{\Delta\theta}{2\pi}\right| \tag{4}$$

when $\Delta\theta/2\pi \ll 1$.

The phase and phase change between the two arms are determined by measuring the power level in each arm and the combined power level of both arms (ref. 8). The power levels are initially set equal to each other, and if the change in power levels and phase change are small the equations of reference 8 can be reduced to

$$\Delta\theta \simeq -\frac{1}{\sqrt{3}}\left(\frac{\Delta P}{P} - \frac{1}{2}\frac{\Delta P_2}{P}\right) \tag{5}$$

If there are standing waves in the plasma region, a correction must be applied to $\Delta\theta$; the correction can be derived from reference 9. Then, by combining equation (5) and the correction, the resulting relation is

$$\int n\,dx = 68.2\,f(VSWR)\left(\frac{\Delta P}{P} - \frac{1}{2}\frac{\Delta P_2}{P}\right) \tag{6}$$

Since the interferometer is an integrating device and the probe yields point measurements, a shape factor must be used to relate the measurements. Thus,

$$\int n\,dx \equiv \bar{n}_{cl}\left[2\int \frac{\bar{n}(r)}{\bar{n}_{cl}}\,dr\right] \tag{7}$$

from which a check of the centerline values of the density can be made. The shape factor $2\int[\bar{n}(r)/\bar{n}_{cl}]dr$ was computed by using the relative values of the current probe measurements.

A schematic diagram of the microwave interferometer is shown in figure 7. A number of methods of power measurement were tried, but the uncompensated bolometer bridge introduced the least noise. Since the bridge was uncompensated, long-term drift due to temperature changes was present, so that the system needed to be continually balanced.

The frequency employed was 9.725 gigahertz with a phase-lock stabilized oscillator. The distance between the horn antennas was 45 centimeters. Because of plating from the thrustor, matched dielectric lenses or dielectric antennas could not be employed. As a result, the system used had standing waves with a resulting voltage standing wave ratio of 1.25.

The low electron density of the thrustor beam ($\approx 10^8$ cm^{-3}) meant a phase-shift measurement of approximately 5×10^{-3} radian for a desired accuracy of 10 percent at the frequency used. This meant that the frequency drift had to be kept to within 0.02 percent and the power level maintained to within 0.2 percent. These tolerances were maintained when a phase-lock stabilized oscillator was used. The small angle change also meant that the dimensions of the interferometer had to be maintained to within 5×10^4 centimeter. This was done by mounting the interferometer on the shock-mounted aluminum H-beam structure shown in figure 4.

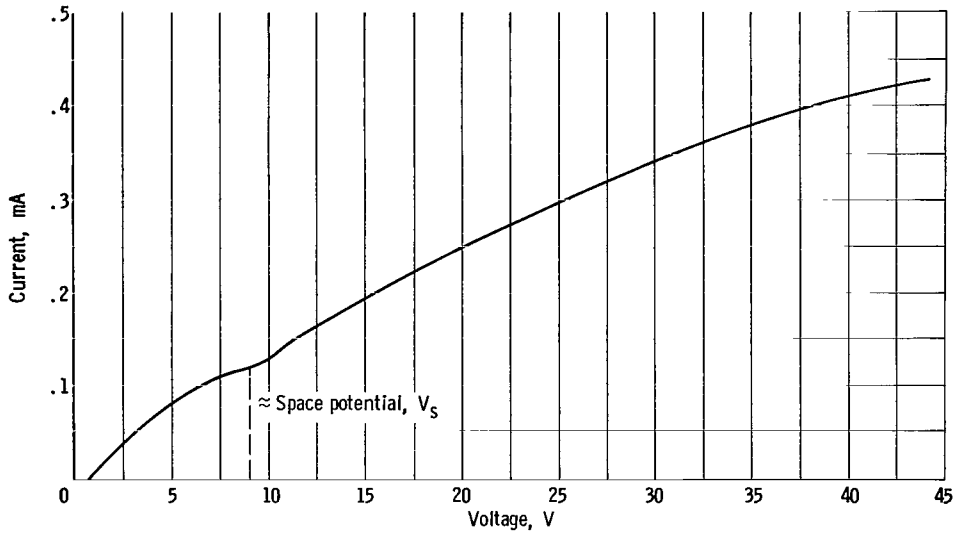

Figure 8. - Langmuir probe current 28.3 centimeters downstream at beam centerline as function of voltage using operating parameters in figure 3.

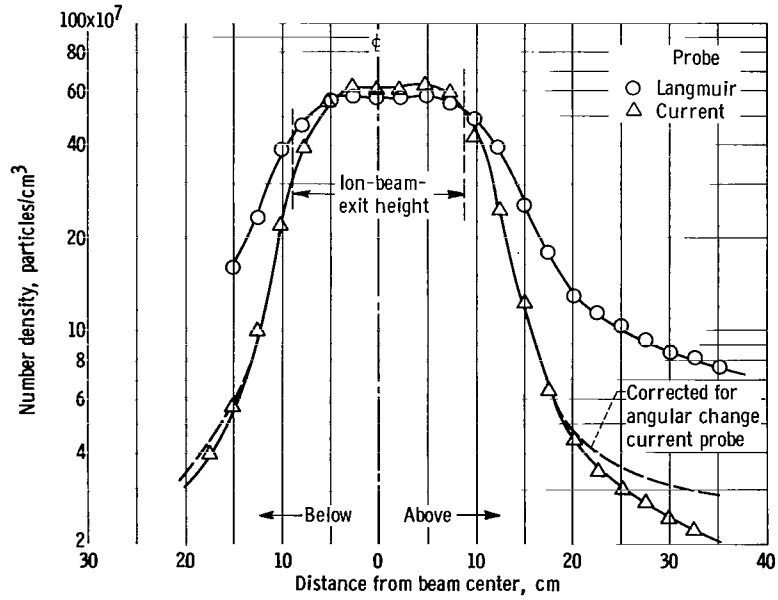

Figure 9. - Profiles of ion-thrustor number-density height taken 26.7 centimeters from thrustor exit.

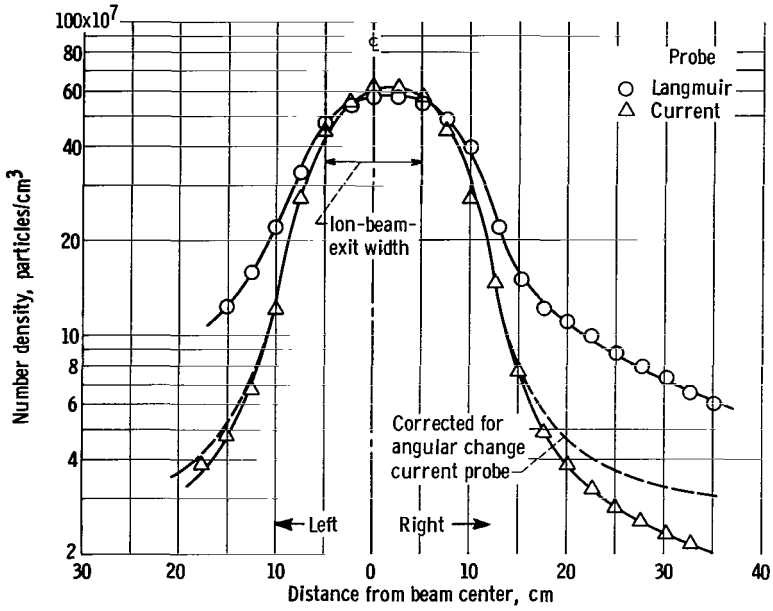

Figure 10. - Profiles of ion-thrustor number-density width taken 26.7 centimeters from thrustor exit.

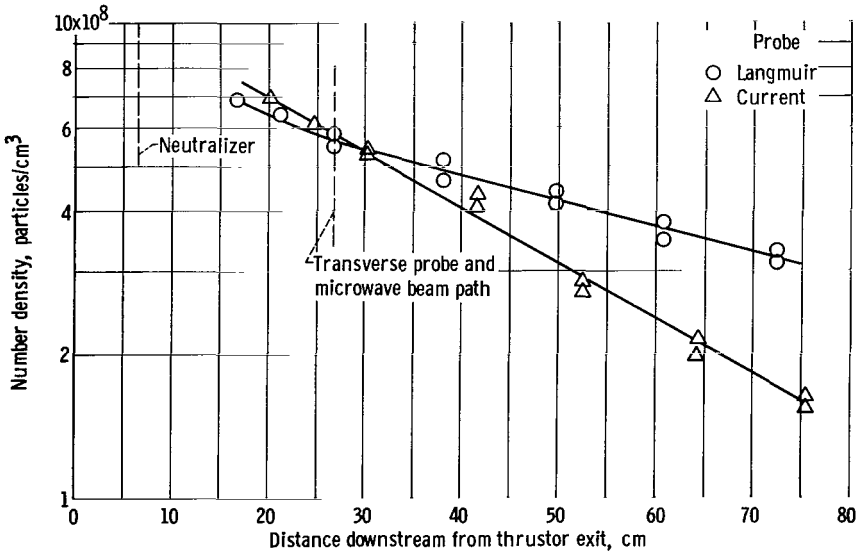

Figure 11. - Downstream number-density profiles near beam centerline.

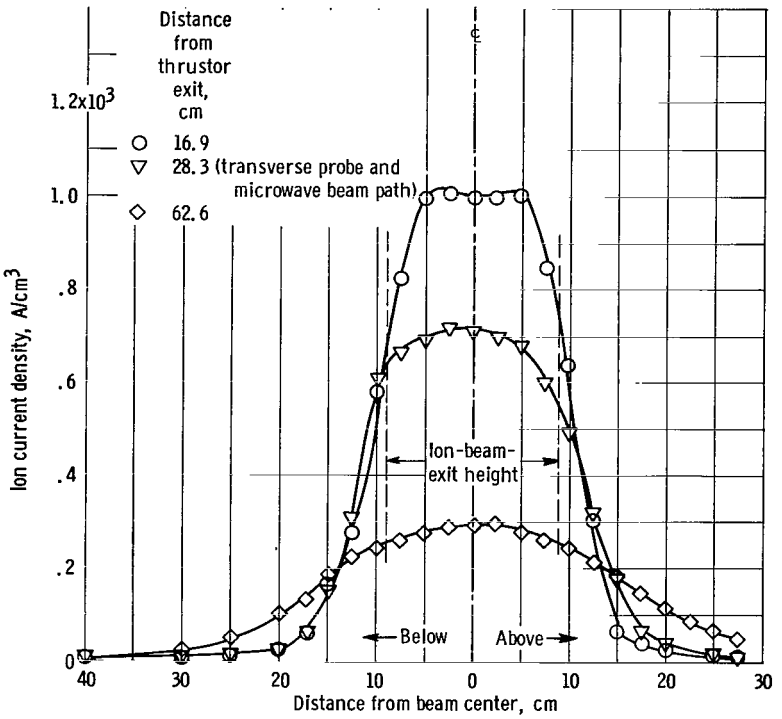

Figure 12. - Downstream ion-current-density profiles. Filament voltage, 30 volts. (Other operating parameters given in fig. 3.)

TABLE I. - COMPARISON OF CENTERLINE CHARGED-PARTICLE DENSITY MEASUREMENT 26.7 CENTIMETERS DOWNSTREAM FROM ENGINE EXIT

Method	Density, particles/cm^3
Langmuir probe	$(5.7\pm1.1)\times10^8$
Microwave interferometer	$(5.4\pm0.6)\times10^8$
Transverse current probe	$(6.2 - 0.5)\times10^8$
Cart current probe	$(5.9 - 0.5)\times10^8$

MEASUREMENTS

Density profiles were taken 26.7 centimeters downstream from the thrustor exit with the transverse current and Langmuir probes (fig. 5). A typical Langmuir characteristic curve taken at the beam centerline is shown in figure 8. By use of equation (2), the electron temperature is estimated to be less than 0.5 electron volt, compared with the 0.26-electron-volt electron temperature in a cesium engine beam (ref. 10). The difficulty of determining V_s makes an accurate electron temperature estimate by this method difficult. Figure 9 gives the number-density profile across the wide-beam dimension, or height, whereas figure 10 gives the number-density profile across the narrow-beam dimension, or width.

Downstream density profiles are taken by means of the current and Langmuir probe cart of figure 6. The results are given in figure 11 over about 65 centimeters of travel. A multicurrent probe cart provides information on the downstream ion-current-density profile or the downstream number-density transverse profile (fig. 12). The density profiles, shown in figure 13, were taken 26.7 centimeters downstream from the thrustor exit with transverse current probes (fig. 5, p. 5) while the thrustor current was varied. A comparison of centerline measurements along with the microwave interferometer results are given in table I.

DISCUSSION OF ERROR

The easiest density measurements to make in the ion-thrustor exhaust are the current probe measurements. Since these measurements are biased so that electrons are rejected, an accurate measurement of ion impingement current, and therefore number density, can be made. Any error is primarily a result of secondary emission from the ion impingement. For stainless steel, the secondary emission in electrons per ion computed from data on related materials in references 11 and 12 for an ion acceleration of 2000 volts is less than 0.1. This secondary emission is reflected as a higher ion-collected current density.

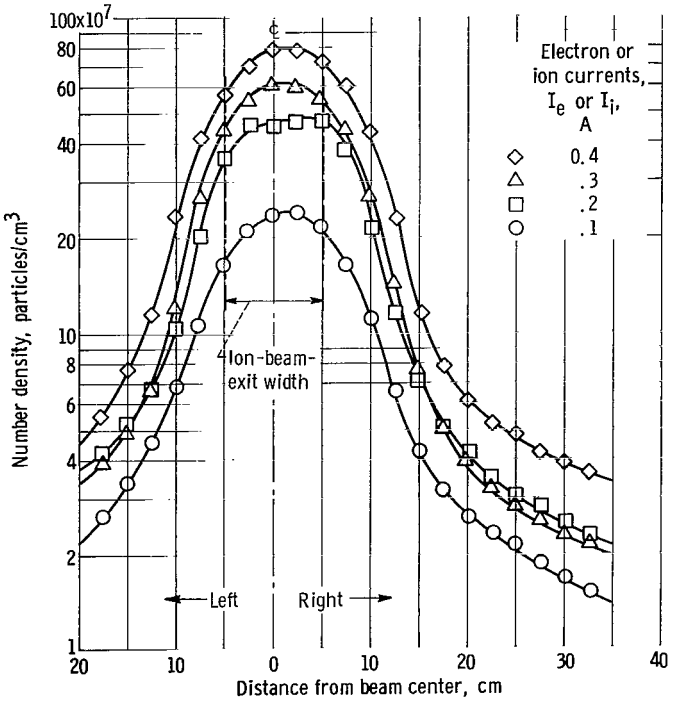

Figure 13. - Profiles of number-density width for various thrustor currents taken 26.7 centimeters downstream from thrustor exit. Data obtained from actuator current probe.

The microwave interferometer measurement is dependent on oscillator frequency stability, constant power levels, a known voltage standing wave ratio, the density profile, and dimensional stability. In this application, the microwave measurement could not be considered more than 10 percent accurate due to these factors.

The Langmuir probe measurements represent the least accurate measurements; an error of about 20 percent could be possible. At the centerline, the current probe, the Langmuir probe, and the microwave interferometer check one another very closely, but in the region where the particle density is below 10^8 particles per cubic centimeter, a large discrepancy between

Langmuir and current-probe results occurs (figs. 9 to 11).

A correction was made to the current-probe measurements to account for the decrease in impingement area with distance normal to the centerline. To make this correction, it was assumed that the ion engine is an array of point sources. Half-current beam width was about 15^{o}. It follows that the source of ions and electrons at the beam edge is in the region of the edges of the array of accelerator holes. The distance normal to the beam centerline from the thrustor hole array edge to the probe centerline is then used in the computation. The corrected values are shown as dashed lines in figures 9 and 10. The correction is not sufficient to account for the discrepancy, however.

The Langmuir probe theory, with orbital motions, is applicable in this region as long as the distribution at the sheath edge is approximately Maxwellian. Ion impingement on the Langmuir probe may vary as a function of position, but when it was measured, no variance was observed. The mean free path is long, so that collisions in the sheath or with background pressure should not have to be considered. The measured current was in the range of 100 microamperes and should not affect the beam appreciably. There may be an excess of electrons at the edges of the beam, but no explanation seems feasible as to why they should be present. The only remaining explanations involve the presence of a slow-moving background ionized gas and/or slowing down of the ion-thrustor beam transversely and longitudinally. Both these explanations are compatible with the resulting measurements.

CONCLUDING REMARKS

The number-density profiles for an ion engine beam were measured (figs. 9 to 13). A comparison of the centerline charged particle density measured by three methods (Langmuir probe, current probe, and microwave interferometer) was made; the results (table I) agreed within ±10 percent. It was demonstrated that both Langmuir probe and microwave-interferometer measurements can be made on low-density plasma sources such as an ion engine.

Lewis Research Center,
National Aeronautics and Space Administration,
Cleveland, Ohio, September 7, 1966,
129-01-07-04-22.

REFERENCES

1. Kaufman, Harold R.: An Ion Rocket with an Electron-Bombardment Ion Source NASA TN D-585, 1961.

2. Kaufman, Harold R.: One-Dimensional Analysis of Ion Rockets. NASA TN D-261, 1960.

3. Byers, David C.; Kerslake, William R.; Grobman, Jack: Experimental Investigation of Heavy-Molecule Propellants in an Electron-Bombardment Thrustor. NASA TN D-2401, 1964.

4. Kerslake, William R.; and Pawlik, Eugene V.: Additional Studies of Screen and Accelerator Grids for Electron-Bombardment Ion Thrustors. NASA TN D-1411, 1963.

5. Mott-Smith, H. M.; and Langmuir, Irving: The Theory of Collectors in Gaseous Discharges. Phys. Rev., vol. 28, no. 4, Oct. 1926, pp. 727-763: also published in Electrical Discharges. Vol. 4 of The Collected Works of Irving Langmuir, C. Guy Suits, ed., Pergamon Press, 1961, pp. 110-115.

6. Huddlestone, Richard H.; and Leonard, Stanley L.: Plasma Diagnostic Techniques. Academic Press, 1965, pp. 113-160.

7. Whitmer, R. F.: Principles of Microwave Interactions with Ionized Media. Pt. 1, Plasma Resonance. Microwave J., vol. 2, no. 2, Feb. 1959, pp. 17-19.

8. Kuhns, Perry: Microwave Interferometer Measurements of Electron-Ion Recombination in Nitrogen, Air, and Argon. NASA TN D-1191, 1962.

9. Stratton, Julius A.: Electromagnetic Theory. McGraw-Hill Book Co., Inc., 1941.

10. Sellen, J. M., Jr.: Investigations of Ion Beam Diagnostics. Final Rep. (NASA CR-53634), TRW Space Technology Lab. Apr. 1964.

11. Kaminsky, Manfred: Atomic and Ionic Impact Phenomena on Metal Surfaces. Academic Press, 1965, pp. 296-329.

12. Gray, Dwight E., ed.: American Institute of Physics Handbook. 2nd ed., McGraw-Hill Book Co., 1963, Ch. 7, pp. 184-203.

"The aeronautical and space activities of the United States shall be conducted so as to contribute . . . to the expansion of human knowledge of phenomena in the atmosphere and space. The Administration shall provide for the widest practicable and appropriate dissemination of information concerning its activities and the results thereof."

—NATIONAL AERONAUTICS AND SPACE ACT OF 1958

NASA SCIENTIFIC AND TECHNICAL PUBLICATIONS

TECHNICAL REPORTS: Scientific and technical information considered important, complete, and a lasting contribution to existing knowledge.

TECHNICAL NOTES: Information less broad in scope but nevertheless of importance as a contribution to existing knowledge.

TECHNICAL MEMORANDUMS: Information receiving limited distribution because of preliminary data, security classification, or other reasons.

CONTRACTOR REPORTS: Technical information generated in connection with a NASA contract or grant and released under NASA auspices.

TECHNICAL TRANSLATIONS: Information published in a foreign language considered to merit NASA distribution in English.

TECHNICAL REPRINTS: Information derived from NASA activities and initially published in the form of journal articles.

SPECIAL PUBLICATIONS: Information derived from or of value to NASA activities but not necessarily reporting the results of individual NASA-programmed scientific efforts. Publications include conference proceedings, monographs, data compilations, handbooks, sourcebooks, and special bibliographies.

Details on the availability of these publications may be obtained from:

SCIENTIFIC AND TECHNICAL INFORMATION DIVISION

NATIONAL AERONAUTICS AND SPACE ADMINISTRATION

Washington, D.C. 20546